Transnational University Limburg is a unique collaboration of two universities in two countries: the University of Hasselt and Maastricht University.

UHASSELT
KNOWLEDGE IN ACTION

www.uhasselt.be
Universiteit Hasselt
Campus Hasselt:
Martelarenlaan 42 | 3500 Hasselt
Campus Diepenbeek:
Agoralaan Gebouw D | 3590 Diepenbeek

UHASSELT
KNOWLEDGE IN ACTION

Maastricht University

Faculty of Medicine and Life Sciences
School for Life Sciences
Master of Biomedical Sciences

Master's thesis

Using Schmidtea mediterranea as an entry point to understand the role of neural signaling in intestinal regeneration

Charlotte Segnana

Thesis presented in fulfillment of the requirements for the degree of Master of Biomedical Sciences, specialization Environmental Health Sciences

SUPERVISOR :
Prof. dr. Werend BOESMANS

CO-SUPERVISOR :
Prof. dr. Karen SMEETS

MENTOR :
Mevrouw Julie TYTGAT

2020
2021

UHASSELT
KNOWLEDGE IN ACTION

Maastricht University

Faculty of Medicine and Life Sciences
School for Life Sciences
Master of Biomedical Sciences

Master's thesis

Using Schmidtea mediterranea as an entry point to understand the role of neural signaling in intestinal regeneration

Charlotte Segnana

Thesis presented in fulfillment of the requirements for the degree of Master of Biomedical Sciences, specialization Environmental Health Sciences

SUPERVISOR :
Prof. dr. Werend BOESMANS

CO-SUPERVISOR :
Prof. dr. Karen SMEETS

MENTOR :
Mevrouw Julie TYTGAT

UHASSELT *Senior internship- 2nd master BMS*

Using *Schmidtea mediterranea* as an entry point to understand the role of neural signaling in intestinal regeneration *

Charlotte Segnana[1], Werend Boesmans[2] and Karen Smeets[1]

[1]Zoology research group, Center for Environmental Sciences, Universiteit Hasselt, Campus Diepenbeek, Agoralaan Gebouw D - B-3590 Diepenbeek
[2]Neuroscience research group, Biomedical Research Institute, Universiteit Hasselt, Campus Diepenbeek, Agoralaan Gebouw C - B-3590 Diepenbeek

*Running title: *The nervous system spills its guts*

To whom correspondence should be addressed: prof. dr. Werend Boesmans, Tel: +3211269165; Email: werend.boesmans@uhasselt.be

Keywords: *Schmidtea mediterranea*, regeneration, intestine, nervous system, RNA interference

ABSTRACT

The intestine is the most highly regenerative organ in the human body, it renews its epithelial lining weekly. To date however, it remains unclear how regenerative tissues are rebuilt in a post-embryonic setting, and how cell cycle dynamics are coordinated in both time and space. The nervous system has been shown to determine intestinal stem cell fate and regulate growth and repair of the epithelium. Now, studying this process in highly regenerative species, like planaria (flatworms), can create new perspectives and in depth understanding of organogenesis, tissue remodeling and wound repair. Their capability to regenerate an entire organ de novo exceeds intestinal epithelial regeneration in vertebrates. Immunohistochemistry was used in combination with fluorescent and confocal microscopy to understand the cellular anatomy and spatial organization of the planarian digestive tract and nervous system. We performed RNA interference to knock-down *choline acetyltransferase*, a transferase enzyme responsible for the synthesis of the neurotransmitter acetylcholine which plays an important role in the vertebrate enteric nervous system. Additionally, the voltage-gated sodium channel blocker tetrodotoxin was used to inhibit nerve cell firing. Neurotoxicity and (gut)regeneration after interference were assessed. Lastly, a general strategy to induce intestinal damage in planaria via ethanol injection was used. Our results suggest that a functioning nervous system is necessary for normal intestinal regeneration. We provide the first evidence of nervous system regulation of intestinal regeneration in *Schmidtea mediterranea.*

INTRODUCTION

Organ growth and tissue remodeling are essential for morphogenesis, and play an important role in maintaining homeostasis during adult life. To date, it remains unclear how regenerative tissues are rebuilt in a post-embryonic setting, and how cell cycle dynamics are coordinated in both time and space (1). The highly proliferative and differentiating nature of the intestinal epithelium, together with the challenging luminal environment it faces, make a strong case for studying regeneration in this setting. The intestinal epithelium's constant regenerative state is supported by a vast pool of stem cells located in the intestinal crypts. This sustains its function as a vital barrier preventing pathogens and toxins from entering the body while, at the same time, allowing the uptake of nutrients, water and electrolytes (2). A 'leaky gut' can have serious consequences such as intestinal inflammation and even neurodegeneration (3, 4). Elucidating the mechanisms of intestinal regeneration will generate invaluable information for evolutionary and developmental biology, and improve the understanding of gastrointestinal disorders and advance regenerative medicine.

To coordinate tissue remodeling inside pre-existing tissues, there must be a high amount of intra-tissue communication. Several lines of evidence indicate

that nerves are necessary for regeneration in both vertebrates and invertebrates (5-8). However, aside from the potential influence of a number of axial polarity cues (9, 10) the mechanisms that regulate differentiation and remodelling of intestinal cells are unknown. Birkholz *et al.* put the nervous system forward as a key regulator of regeneration in flatworms in his recent review (11). Furthermore, in a recent study Bischof *et al.* found that factors driving the repatterning are not diffusing through the mesenchyme but are transported along axial structures, such as the ventral nerve cords (12). These studies indicate that finding the mechanistic links can clarify the role of the nervous system in regeneration. However, if and how neural signaling directs intestinal regeneration is not clear. In a 2012 article, Forsthoefel *et al.* provides evidence for a potential niche-like role of intestinal phagocytes in the regulation of neoblast dynamics (13). Hence, there are still a lot of ambiguities concerning the role of the nerves in the regeneration process.

In vertebrates, a dedicated nervous system located within the gut wall autonomously controls gastrointestinal functions such as motility and absorption (14). Interestingly, this so-called enteric nervous system (ENS), has also been shown to determine intestinal stem cell fate and regulate growth and repair of the epithelium (6, 15). Studying this process in highly regenerative species, such as planarians (flatworms), can create new perspectives and deepen our understanding of organogenesis, tissue remodelling and wound repair, because their capability to regenerate an entire organ *de novo* exceeds intestinal epithelial regeneration in vertebrates. Together with its rather simple anatomy with few tissue layers and cell types, the planarian model is a promising system to elucidate the molecular and physiological mechanisms of intestinal regeneration and morphogenesis, and the role of the nervous system in these processes.

One of the most prominent unanswered questions today is: what role does the nervous system play in intestinal regeneration? Uncovering intestinal regeneration can have significant biomedical relevance, for a vast number of diseases or gastrointestinal disorders are associated with luminal cell malfunctions, defects or failures.

EXPERIMENTAL PROCEDURES

Schmidtea mediterranea cultivation – Asexual strains of the species *S. mediterranea* were used. They were kept in the established cultivation medium (1.6 mM NaCl, 1 mM $CaCl_2$, 1 mM $MgSO_4$, 0.1 mM $MgCl_2$, 0.1 mM KCl, and 1.2 mM $NaHCO_3$). The planarians were continuously maintained in the dark at a temperature of approximately 20°C. Once a week they were fed with veal liver. Prior to the measurements, animals were starved for at least 7 days to avoid food-related effects.

Ethanol injection – To induce local damage to the intestinal epithelium animals were injected with 15% ethanol (EtOH) directly into the intestine (pre-pharyngeally). Controls were injected with milli-Q water. Suitable EtOH concentration was determined via a dilution series (10%, 25%, 50%, and 75%). To inspect the degree of intestinal damage EtOH-injected worms were visually observed after EtOH injection and hematoxylin and eosin (HE) stained. Assessment on intestinal integrity and stem cell proliferation was executed via 6G10 and H3P staining at day zero and three respectively.

TTX exposure – Planaria were exposed to a pharmacological neurotoxin, tetrodotoxin citrate (TTX), for a period of 24h or 48h (10 µM, 100 µM, 500 µM and 1 mM). After initial 48h exposure animals were cut pre-pharyngeally and allowed to regenerate in the TTX solution. The regenerative capability was studied by measuring differences in blastema sizes at 7 and 14 days post cutting, compared with control samples. On day 14 animals were fixed and staining was performed for the nervous system and intestinal muscle.

RNA interference – Double-stranded RNA (dsRNA) for Smed-chat was synthesized (forward primer: TAGACAACATTCGTGCGGCT, reverse primer: CTGCGACATGACTCCTCCAA). The GOI sequence was consulted on two databases, NCBI and Planmine. Primer3 (version 4.1.0) was used for RNAi primer design. Primary PCR was performed followed by gel electrophoresis. The PCR product was cut out of the gel and purified (GeneJET PCR Purification Kit®, Thermo Scientific). To make dsRNA probes for RNAi purified PCR products were reversed transcribed

with the T7 RiboMAX™ Express RNAi System (Promega). Purified RNAi probes were diluted to 1000 ng/µl and stored at -20°C.

The injection schedule consisted of 3 consecutive injection days per week for 2 weeks or for 1 week. Injections were done using the Nanoject II (Drummond Scientific, Broomall, PA, USA) and consisted of three times 32 nl containing 1 µg/µl dsRNA for 2 week injections and three to six times 32 nl (1 µg/µl dsRNA) for 1 week injections. Controls were injected with milli-Q water. On day 4 of the last injection round, planarians were cut pre-pharyngeally to induce regeneration.

Blastema measurements – The effects of RNAi with Smed-chat on the ability to restore the regenerative capacity were studied by measuring differences in blastema sizes on 7, 10 and 14 days post cutting, compared with control samples. Blastema areas were quantified using ImageJ (version 1.53a) on digital micrographs acquired with a Nikon DS-Ri2 digital camera mounted on a Nikon SMZ800 stereomicroscope. Photos and measurements were taken in triplicate per individual. The blastema area measurements were normalized against the total body area of the worm. Worms were also scored according to their photoreceptor (eye) development. Therefore, the presence of the eyes (2, 1 or 0 eyes) on 10 or 14 days post cutting was documented.

Ganglia development measurements – Samples were stained with the anti-synorf antibody which labels the central nervous system. The relative brain ganglia widths were calculated. For this the brain width was normalized against the head width. Measurements were performed with ImageJ (version 1.53a) on digital images acquired with a Nikon DS-Ri2 digital camera mounted on a Nikon SMZ800 stereomicroscope.

Motility assay – Planarian motility was assessed at day 7 post cutting with a two-minute planarian locomotive velocity (pLMV) assay conducted according to the procedure described by Lowe *et al*. (16). Briefly, a petri dish was placed on a 0.5 cm grid, and the pLMV was quantified as the cumulative number of lines crossed or recrossed by the planarian head or tail fragment in 2 min, excluding 20 seconds of acclimatization.

Whole-mount Immunohistochemistry – In order to study the intestinal cellular environment several types of intestinal cells, nerve cells, enteric muscle, and stem cells were visualized. All antibodies that were used are presented in Table 1, with concentrations. Small animals, 2-4 mm, were selected for protocols. Animals were killed in 2% HCl or 5% NAC for 5 minutes. After rinsing with PBS, formaldehyde-based fixation took place (15 minutes), followed by PBSTx (PBS + 0.3% Triton X-100) rinses and bleaching in 6% H_2O_2 aqueous or MeOH (dehydrated) overnight. The following day samples were rehydrated (if necessary) and rinsed with PBSTx. Additional reduction and/or proteinase K steps were included in several protocols. Blocking for 1h to 8h in 1% BSA/PBSTx was followed by addition of primary antibody diluted in 1% BSA/PBSTx, incubation overnight at 4°C. After thoroughly rinsing with PBSTx samples were again blocked in 1% BSA/PBSTx, followed by addition of the second antibody diluted in 1% BSA/PBSTx. After final washing steps with PBST, samples were mounted in Shando Immu-Mount (Thermo Fisher Scientific) and analyzed with a Nikon eclipse i80 fluorescence microscope equipped with a Ds-Ri2 camera and confocal microscope Zeiss LSM900 KMAT, photometrics 95B). Detailed protocols are provided in supplementals and any deviations from this protocol are mentioned with the experiments or indicated in additional supplements.

The following primary antibodies were used: rabbit anti-phospho-histone H3 (1:1000; Cell Signaling Technology, Danvers, MA), mouse 3C11 anti-synorf (1:50, Developmental Studies Hybridoma Bank, developed by Buchner E.), anti-phosphotyrosine (1:50, Cell Signaling Technology, Danvers, MA), 2C4-C2 (1:1000), 1H6-E9 (1:1000), 6G10-2C7 (1:50), and 6C8-A2 were deposited to the DSHB by Zayas, R.M. (DSHB Hybridoma Product. Secondary antibodies (Invitrogen™, Massachusetts, USA) were used at a dilution of 1:400 (goat anti-mouse Alexa Fluor 488) or 1:500 (goat anti-rabbit Alexa Fluor 568).

Immunohistochemistry on coupes – To avoid dessication of the samples, a 'humid chamber box' filled with water and a coverslip were used. After thorough rinsing with PBS, samples on slides are blocked in 1% BSA/PBSTx over 2h. The primary

antibody dissolved in 1% BSA/PBSTx is added and incubated overnight (4°C). Next day proceeds with thorough PBS washing steps, followed by incubation with secondary antibody for 3h at RT. Before mounting samples are washed repeatedly with PBS. Samples were mounted in Shando Immu-Mount (Thermo Fisher Scientific).

Imaging and image processing – Immunolabeled samples were imaged on a Nikon eclipse i80 fluorescence microscope equipped with a Ds-Ri2 camera and confocal microscope (Zeiss LSM900 KMAT, photometrics 95B). Where appropriate, adjustments to brightness and contrast were applied identically to allow comparison of immunolabeling.

Statistical analysis – Groups were compared using a one-way analysis of variance (ANOVA) followed by a Tukey HSD post-hoc test for multiple comparisons. Normality was tested with the ShapiroWilk test. If the assumptions of normality were not met, transformations of the data were applied (Log, Square root, 1/x and ex). If data were not normally distributed after transformations the non-parametric Kruskal-Wallis test was computed, followed by the pairwise wilcoxon test for multiple comparison. Alternatively, for comparing two groups the unpaired two-samples t-test was applied. Normality was tested with the ShapiroWilk test and the F-test was used to test for homogeneity in variances. All statistical analyses were performed using RStudio 4.0.0 (Rstudio, Inc.). p-values <0.05 were considered significant.

RESULTS

Mapping of planarian neural and intestinal tissues – To optimize immunostainings for intestinal tissue and neural structures we opted for one of two chemical treatments commonly used to relax planarians and remove their mucus secretions prior to fixation: hydrochloric acid (HCl) and N-Acetyl-L-cysteine (NAc). Various fixatives were also considered and tested based on literature recommendations or supplier information. Furthermore, we varied the duration and concentration of the antibody and blocking solution. Immunolabeling for intestinal stem cells (6C8), the nervous system (1H6), the gut (6G10 anti-phosphotyrosine), and goblet cells (2C4) were optimized. A general overview is provided in supplemental table 1 and figure 1.

The monoclonal antibody anti-6G10 labels the subepidermal, pharyngeal and intestinal muscle fibers of *S. mediterranea* (17). Several fixation protocols in combinations with varying antibody dilutions were tested (table 1). A formaldehyde-based fixation (Nac-FA-Me) with a 1:50 dilution resulted in a specific staining with low background in whole-mount samples. When imaging whole-mount anti-6G10 immunostained samples a large magnification is needed (40x) on a confocal microscope, in order to image the deeper tissue layer in which the intestine is located (fig. 1B). The planarian intestine is highly branched and convoluted, therefore using a confocal microscope yields the possibility of focussing on different tissue levels which creates a 3D-like overview of the intestine (fig. 1B3). Intestinal regeneration can be further investigated by utilizing immunofluorescence to detect the marker phosphotyrosine, which is found on the apical surface of intestinal epithelial cells, effectively labeling the intestinal lumen as visualized in figure 1C (18, 19). For the anti-phosphotyrosine antibody a HCl-methacarn-Me fixation with longer blocking periods performed best (Table 1). Proteinase K treatment did not improve the signal, on the contrary this produced poor results with high background.

Ross *et al.* hypothesized that anti-6C8 (6C8) immunolabeling identifies cells that are programmed to become intestinal cells in the mesenchyme and are in the process of incorporating into the intestinal epithelium, because 6C8 labels a cell population that is near to and inside the intestinal musculature border (17). To enhance the labeling of intestinal stem cells several fixation protocols with varying blocking periods were tested (Stable 1), but we were not able to settle on a high quality staining (fig. 1D). A NAc-FA fixation with short blocking produced the most promising results. From our experiments 2C4 strongly labels a broad network located closer to the epidermis, but also the

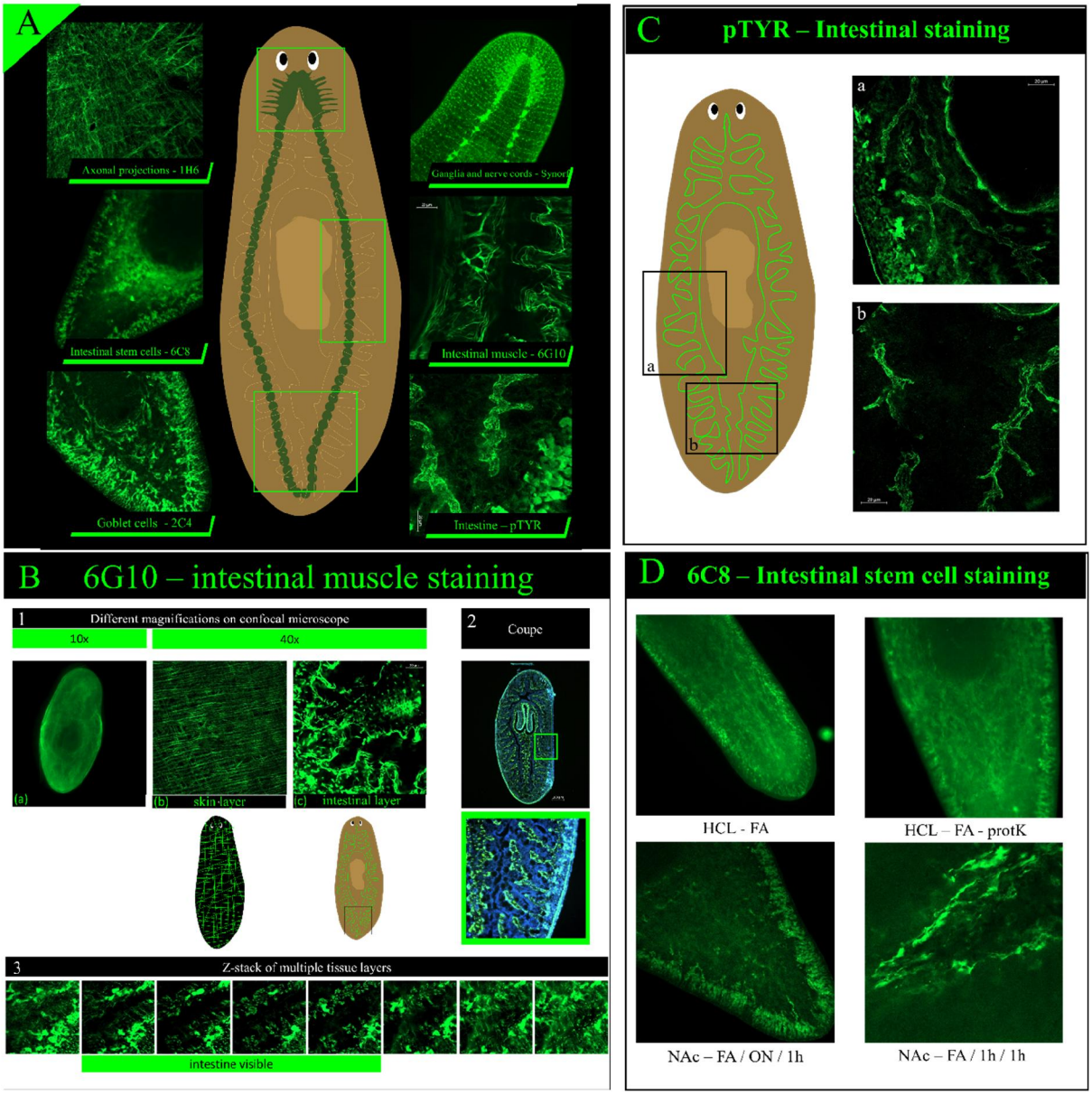

Figure 1: Overview figure of immunostainings. (A) Confocale images of stainings for the nervous system, intestine, intestinal muscle,stem cells, and goblet cells. The green squares corresponds to the confocal images shown left and right. **(B)** 6G10 intestinal muscle staining optimization. (1) Shows differences in images aquired based on magnification with (2) being a high magnification focussed on the subepidermal muscle wall composed of circular, longitudinal, and diagonal fibers and (c) on the deeper tissue layer where the intestine lies. (2) Overview images of 6G10 staining can be aquired by staining coupes. (3) A z-stack shows the different tissue layers. **(C)** Anti-phosphotyrosine antibody labels intestinal epithelial cells. **(D)** Different fixation protocols tested for 6C8 staining optimization.

central region where the intestine is located gives a clear signal. Because 2C4 marks large neuronal cells surrounding the pharynx as well as cells within the gut, the protein recognized by 2C4 may be strongly expressed in cells engaged in secretion, as suggested by Ross *et al.* (17).

Labeling with an antibody for 1H6 was used to visualize axonal projections in both the central and peripheral nervous systems (fig. 1A). To stain whole-mount samples the recommendations by Ross et al. (17) were followed and a Nac-FA-Red-Me-ProtK fixation was successfully applied (STable 1).

Injection with ethanol induces local damage to intestinal epithelium – In order to study intestinal regeneration in a more general 'local damage' setting animals were injected with an ethanol (EtOH) dilution series (10%, 25%, 50%, and 75%). The highest concentration (75% EtOH) was lethal. With a 50% EtOH injection animals visibly suffered and bulged their pharynx out. These findings were confirmed with the H&E staining (fig. 2B). For further experiments a sublethal condition, where the planaria showed no visible damage, was chosen (15% EtOH). Alternatively, the degree of damage after EtOH injection was assessed via 6G10 immunolabeling of the gut muscle wall. EtOH-injected animals showed visible signs of damage inside the intestine compared to controls as indicated in figure 2C (red arrows). Also in the tissue surrounding the intestine on the lateral sides holes can be seen (fig. 2C a, red 'X'). Overall gut structure and integrity appears to be preserved after EtOH injection.

Besides intestinal regeneration, the stem cell proliferation was examined using immunohistochemical H3P staining. To study the repair process samples were fixed at day three post cutting. The average number of proliferating stem cells did not significantly differ between control and EtOH-injected worms (fig. 2D). A slightly decreasing trend was observed.

Knock-down of choline acetyltransferase results in impaired regeneration – The planarian nervous system makes use of a diverse range of neurotransmitters, including acetylcholine (ACh). Knock-down of this enzyme via RNAi resulted in neurodegenerative effects after 10 days of regeneration. With immunolabeling for the central nervous system (anti-synorf) a decreasing trend in ganglia regeneration was observed in both head and tail fragments compared to controls (fig. 3A). 50% of the RNAi head fragment's cephalic brain ganglia were separated and already started showing signs of tissue breakdown at the anterior end (fig. 3C a, red arrow). Notable from day 7 on was the limited motility of RNAi-treated head fragments. The motility assay, based on the number of lines crossed in a petri dish (fig. 3B b), clearly showed that head and tail fragments were significantly ($p < 0.001$) worse compared to control samples (fig. 3B). Additionally, RNAi-head fragments performed significantly worse than RNAi-tail fragments ($p < 0.05$).

Knockdown of choline acetyltransferase after 2 rounds of RNAi resulted in a reduction in blastema formation measured at day 7 and 10 post cutting (fig. 4A). This reduction in regeneration was most notable in the tail fragments ($p < 0.001$). For the head fragments a similar trend was observed at 5 dpa, although this was not significant. After 5 days of regeneration two out of ten head samples showed bulge formation. After 7 days this trend continued with five out of ten head samples being disformed and one dead (fig. 4Ab). From day 10 all surviving head fragments (eight out of ten) had formed a secondary blastema on the apical side and lost one or both eyes (fig. 4D, red arrowheads). This is consistent with the lesions observed with the anti-synorf staining on head fragments mentioned before (fig. 3C). Alternatively, tail fragments were visually less affected. Notable was a narrower head regeneration in tail (fig. 4E). All tail fragments were able to regenerate their eyes.

To confirm our findings and investigate intestinal regeneration after choline acetyltransferase silencing a second RNAi experiment was started, but a single injection week was applied here. 5 dpa no significant difference in head or tail fragments compared to controls was observed (fig. 4B a). But at 10 dpa tail fragments clearly showed reduced blastema formation ($p < 0.01$, fig. 4B ab). In other words, the reduced blastema formation for the 1 week and 2 weeks injection protocol was preserved (fig. 4), most notably in the tail fragments. But, when inspecting neuroregeneration alternative

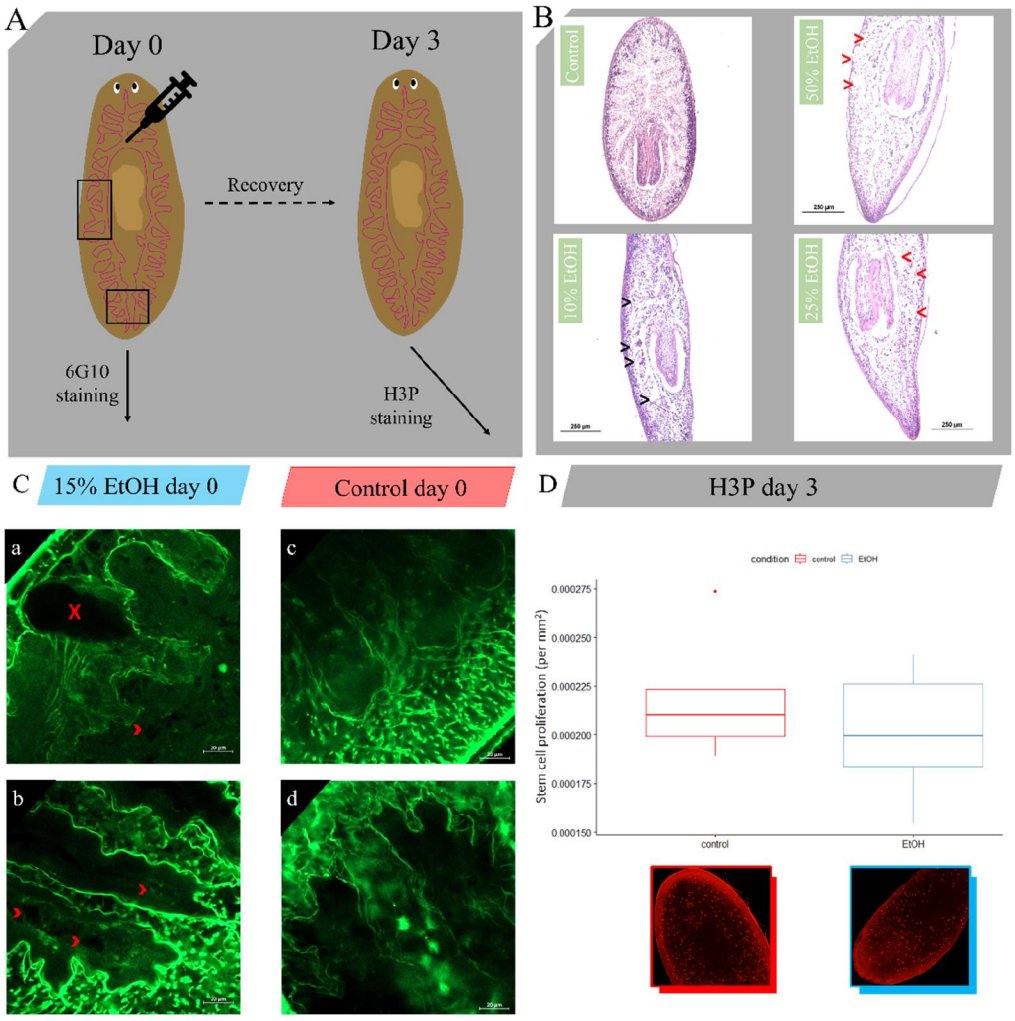

Figure 2: Injection with ethanol induces local damage to intestinal epithelium. (A) The experiment setup is displayed in the grey box, indicating the injection site and timing. The black square corresponds to the images shown in (C). (B) H&E staining of control and EtOH-injected planaria. Black arrowheads indicate persevered intestinal branch, red arrowheads indicate damage. (C) 6G10 staining of intestinal muscle at day 0, red 'X' indicates large lesion in mesenchyme, red arrowheads indicate lesions inside the intestine. (D) H3P-positive cells (per mm²) in adult animals after 3 days of recovery from EtOH injections. The results are expressed as the mean ±SD of 8 samples per condition.

results were obtained. RNAi-treated tail fragments had a larger brain ganglia width at day 11 post cutting compared to control samples (fig. 3D). Finally, intestinal regeneration was also studied via the 6G10 intestinal muscle staining (fig. 5). 13 dpa there is apparent disparity between controls and RNAi-samples. This is best seen in the posterior and lateral images (fig. 5B, D). Secondary branch formation appears underdeveloped in RNAi-treated planaria (fig. 5 purple arrowheads). In one out of 10 samples we observed abnormal fusion of the two posterior branches (fig. 5B d, red arrowhead).

Treatment with the pharmacological neurotoxin tetrodotoxin impedes intestinal regeneration – Tetrodotoxin (TTX) selectively blocks sodium channels and thereby inhibits action potential firing. To determine the effective dose of TTX a dilution series, based on literature findings, was set up. Planaria were exposed to 10 µM, 100 µM, and 1 mM for 48h. After two days of TTX exposure planaria were cut and allowed to regenerate in the TTX solution for seven days. In tail fragments all TTX concentrations resulted in a significant reduction in blastema formation, except 100 µM (10 µM, $p < 0.05$; 1 mM, $p < 0.001$; fig.

6A). In head fragments this inversely proportional trend of concentration and blastema size was also observed (fig. 6A). Here, the highest TTX exposure resulted in a significantly smaller blastema area, compared to the non-exposed worms ($p < 0.05$).

Based upon the results of the dilution series experiment a concentration of 500 µM TTX was selected to further investigate intestinal regeneration. Intact flatworms were incubated in 500 µM TTX for 24h. After this incubation they were cut, followed by 13 days of regeneration in the TTX solution. All individuals survived in the TTX solution for the entire experiment. Average blastema size was noticeably reduced in TTX exposed flatworms (heads, $p < 0.01$; tails, $p < 0.001$; fig. 6B), indicating impaired regeneration. Furthermore, almost no TTX exposed flatworms were able to regenerate their eyes (fig. 6D). Because tetrodotoxin is a neurotoxic compound cephalic ganglia regeneration was also assessed. However, we didn't see an effect of any TTX concentration on neuroregeneration (fig. 6C) when measuring brain size as depicted in (fig. 3E). But although ganglia in TTX-exposed worms do not appear smaller based on width, they do appear to be shorter (fig. 6C red arrows). Intestinal regeneration was examined visually based on the 6G10 immunostaining. Animals were fixed at day 13 postcutting, when the pharynx and nervous system hadcompletely regenerated. Restoration of intestinal polarity, visualized by the 6G10 marker, was reestablished after 13 days in head fragments. Elongation of the posterior branches was observed in control and TTX-exposed samples. However, TTX-exposed head fragments clearly lacked

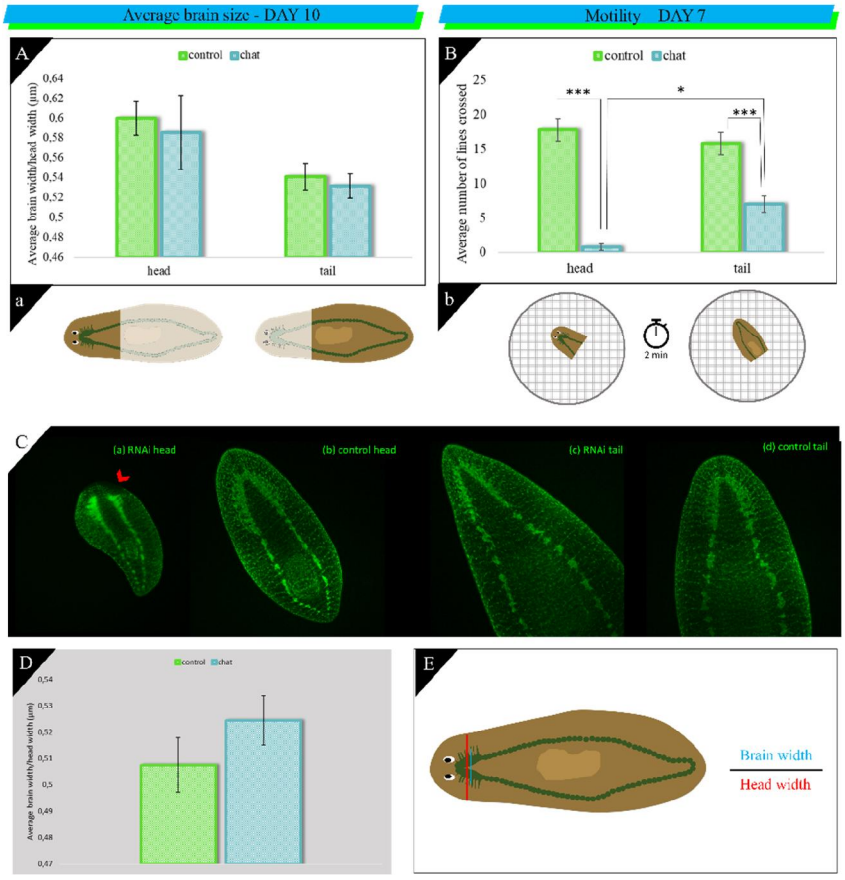

Figure 3: Knock-down of choline acetyltransferase has neurodegenerative effects. Gray graph is data 1 week chat-probe injection and white graphs are 2 week chat-probe injection. (A) Average brain width (mean ±SE) of 10 replicates/ condition after 10 days of regeneration. The amputation setup is displayed in (a), indicating the amputation sites and regenerating blastemas. (B) Motility of head and tail fragments (mean ±SE) of 10 replicates/ condition after 7 days of regeneration, with the experimental setup displayed in (b). (D) Pictures show the immunohistochemical staining of the nervous system (anti-synapsin). Red arrowhead indicates lesion. (E) Average brain width (mean ±SE) of 12 replicates/condition at 11 dpa. (F) The brain size measurements are displayed at the bottom right, indicating the head width (red line) and the brain width (blue line). Statistical significance is indicated by: *: $p < 0.05$; **: $p < 0.01$; ***: $p < 0.001$

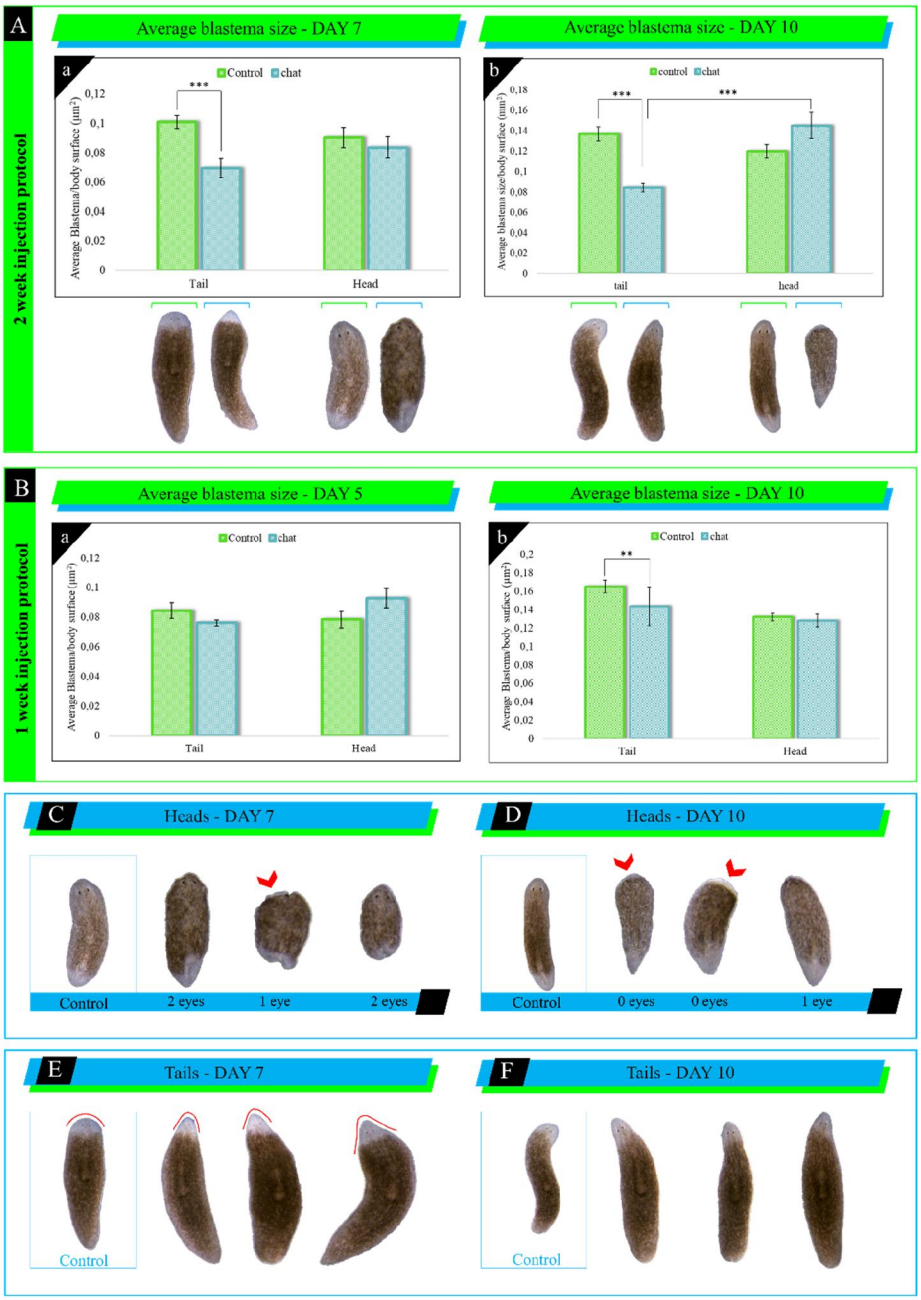

Figure 4: Knock-down of choline acetyltransferase results in impaired regeneration. (A) Mean blastema sizes ±SE of 10 replicates/ condition at day 7 and 10 of regeneration after 2 weeks of chat-probe injection. (B) Mean blastema sizes ±SE of 20 replicates/ condition at day 5 and 10 of regeneration after 1 week of chat-probe injection. (C) Regenerating head fragments at 7 dpa. Red arrows indicate a second blastema on the head corresponding with loss of eyes. (D) Regenerating head fragments at 10 dpa. Red arrows indicate second blastema on head corresponding with loss of eyes. (E) Regenerating tail fragments at 7 dpa. Red lines indicate second blastema head shape. (F) Regenerating tail fragments at 10 dpa. Statistical significance is indicated by: *: $p < 0.05$; **: $p < 0.01$; ***: $p < 0.001$

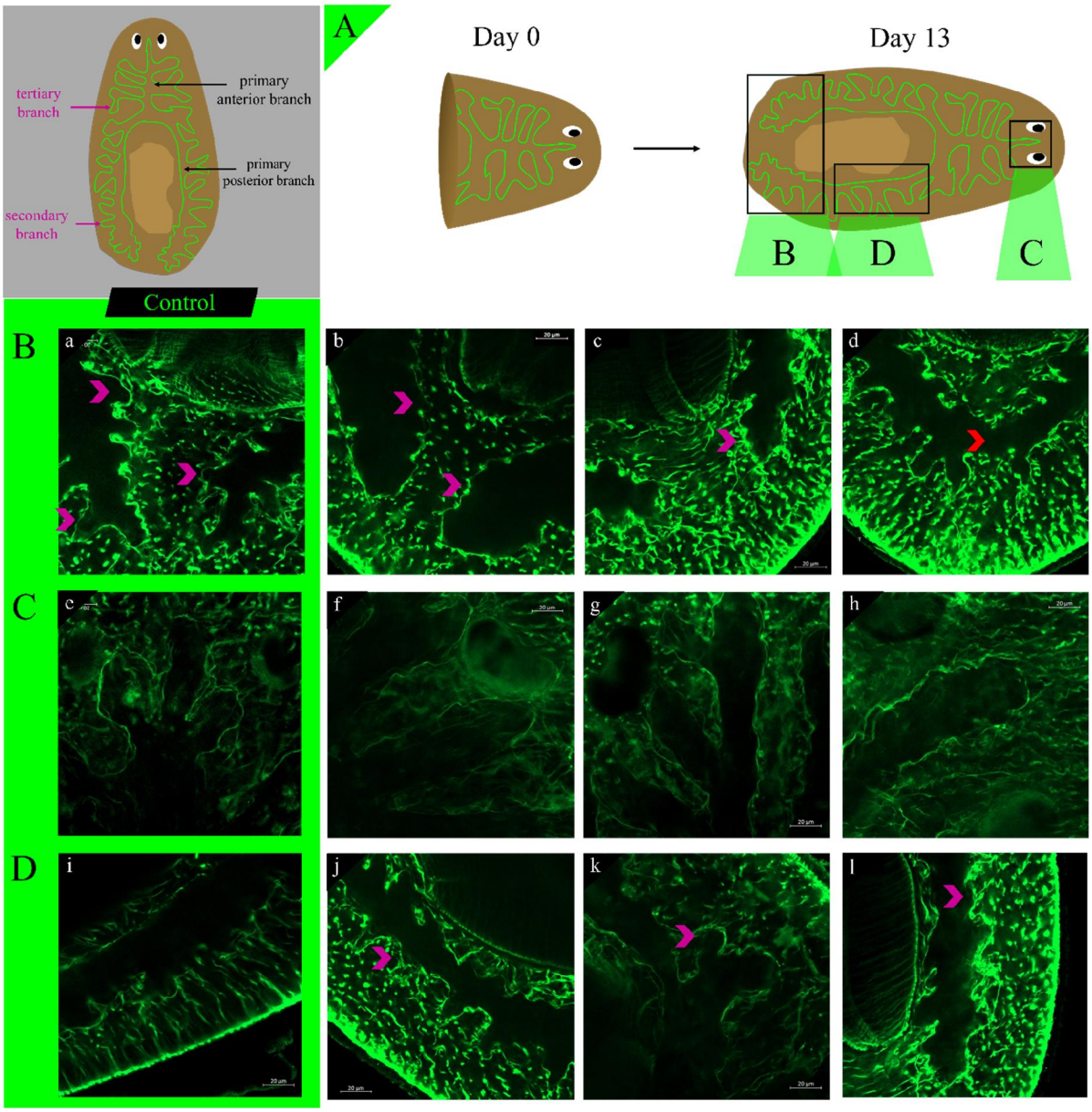

Figure 5: choline acetyltransferase silencing impairs intestinal regeneration. The branching structure of the intestine is depicted in the light gray box. (A) The experiment setup is displayed at the top, indicating the amputation sites and timing. The black squares correspond to the images shown in row (B), (C), and (D). Confocal images of control (green box) and RNAi 6G10-stained samples: row B shows posterior (tail) part, row C shows head (with eyes) part, and row D shows the lateral (side) part. Purple arrowheads indicate secondary branches (or lack thereof).

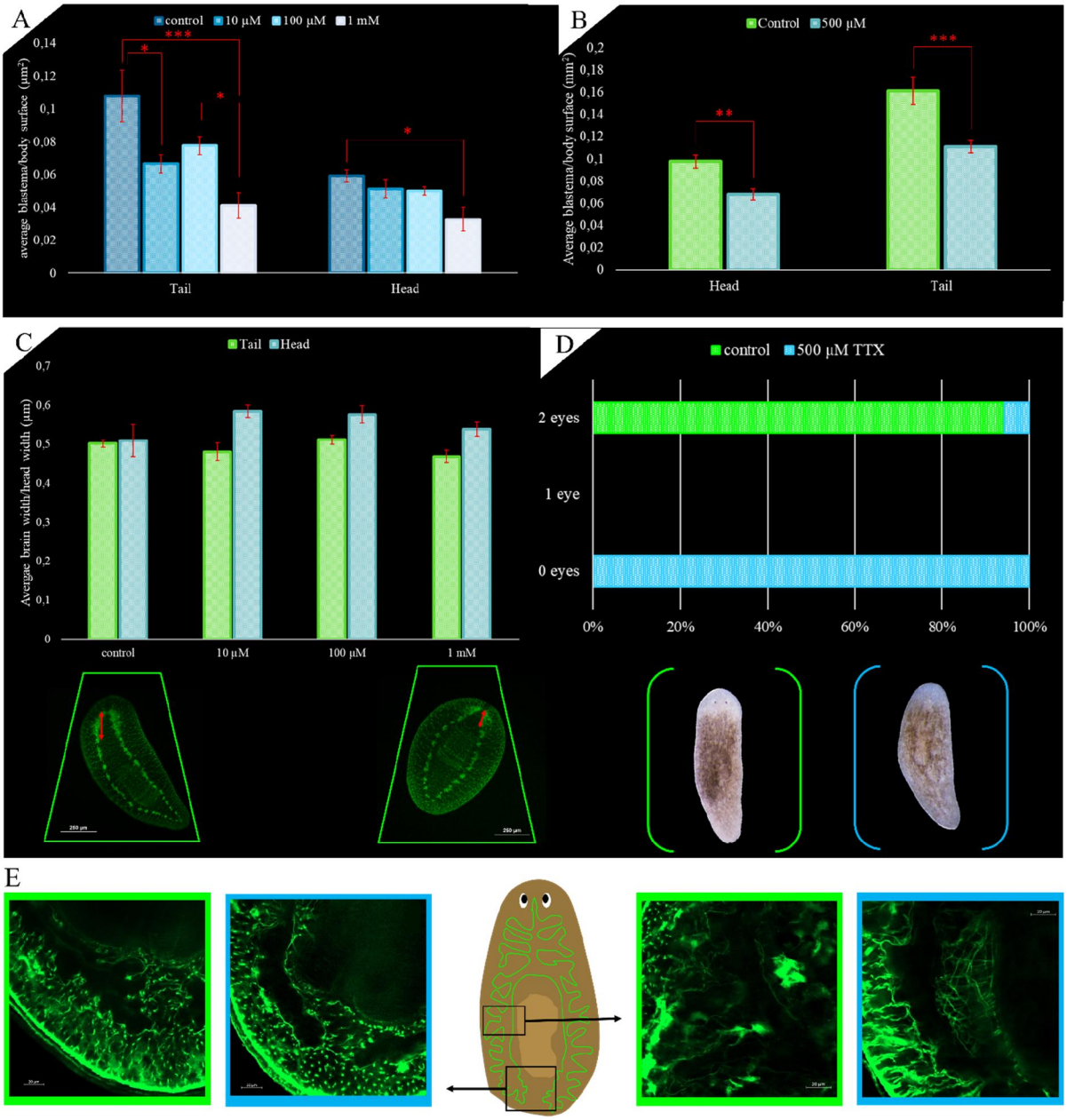

Figure 6: Treatment with the pharmacological neurotoxin tetrodotoxin impedes intestinal regeneration. (A) Mean blastema sizes ±SE of 5 replicates/ condition, in tails and heads. Exposure to 10 µM, 100 µM, and 1 mM TTX; measurements at 7 dpa. (B) Mean blastema sizes ±SE of 17 replicates/ condition, in tails and heads. Exposure to 500 µM TTX; measurements at 10 dpa. (C) Relative brain width at 7 dpa exposure to 10 µM, 100 µM, and 1 mM TTX. Pictures underneath show the immunohistochemical staining of the nervous system (anti-synapsin). Measurements were performed in at least 4 samples per condition. (D) Appearance of the eyes in tail fragments. Green bars are controls (10 samples); blue bars are 500 µM TTX exposed (17 samples). The colored brackets correspond to colors of control and exposed samples in graph above. This graph represents the same samples as used to measure the blastemas in (B). (E) 6G10-stained planaria exposed to 500 µM TTX at 13 dpa. The black squares correspond to the images shown left and right. Confocal images of control (green box) and chat RNAi fragments (blue box.) Statistical significance is indicated by: *: $p < 0.05$; **: $p < 0.01$; ***: $p < 0.001$

secondary and tertiary branch formation at the posterior side (fig. 6E left panel). Additionally, the newly formed posterior primary branches extend less far compared to the control samples. On the lateral side branches also seemed to lack the extent of secondary and tertiary growth compared with control samples (fig. 6E right panel). Anterior branch growth appeared unaffected.

DISCUSSION

In vertebrates, a dedicated nervous system located within the gut wall autonomously controls gastrointestinal functions such as motility and absorption (14). This enteric nervous system (ENS), has also been shown to determine intestinal stem cell fate and regulate growth and repair of the epithelium (6, 15). Taken together the recent data from both vertebrate and invertebrate studies suggest that gut regeneration relies on nerve cell signaling. The molecular mechanisms involved in the neural control of intestinal regeneration, however, remain to be explored.

In this study *Schmidtea mediterranea* was used as an entry point to understand the role of the nervous system in intestinal regeneration. Studying how neural activity drives tissue remodeling in a highly regenerating context is a pioneering approach, able to yield new elementary insights in gut morphogenesis and organogenesis. Traditional models of the intestinal epithelium include epithelial cancer cell lines such as Caco-2 or HT29 cells, which give only partial representations of a healthy intestinal epithelium. These lines have a limited capacity to reflect the many epithelial phenotypes, each of which serves a distinct role in terms of intestinal health and barrier integrity (20). Invertebrate animal models possessing regeneration ability in such tissues provide a viable alternative system for study.

To perform an initial screening for investigating the reliance on the nervous system for proper intestinal regeneration, we opted for a multi-interference strategy. On one hand, we functionally interfered with specific targets: the pharmacological agent TTX was used to block voltage-gated sodium channels in the nervous system and RNA interference was used for transcriptional silencing of choline O-acetyltransferase. On the other hand general damage was induced in a simple and useful way via ethanol injections. A 15% ethanol injection clearly induced damage to the planarian intestine, as shown with the HE and 6G10 staining. EtOH is known to interfere with the nervous system (21, 22), although we can not exclude that the observed damage results from the direct effect of EtOH to tissues. This method can prove to be an effective way to study the repair process in *S. mediterranea.* Lowe *et al.* found that exposure to 1% ethanol impedes movement and light avoidance behavior during head regeneration, and induces dose-dependent mortality and motility attenuation (16). Besides, in a 2010 article Stevenson showed that a short 1-hour treatment with 3% ethanol inhibited movements of *S. mediterranea* with full recovery. Furthermore, he concluded that EtOH treatment did not interfere with regeneration, or damaged epithelial cells (as assayed by H&E staining) (23). This is inconsistent with the results of Lowe *et al.* and this study. A notable difference however between the two mentioned studies and our experiment is the exposure route, being through the medium or injection respectively. In general, after wound induction or amputation an initial peak in mitotic numbers occurs after 4-12 hours, followed by a second peak in mitotic numbers 2-4 days later, more strongly around the wound site (24, 25). We observed no recovery 3 days post-injection, which we would expect. This may be because we have to look at other time points, or because EtOH interferes with the nervous system and thereby hinders recovery. (24, 26, 27). Moreover, EtOH has been demonstrated to alter the firing activity of mouse brains, as well as to lower the excitability of neurons in the central nervous system and block synaptic currents in mammals (28). The planarian central neural system shares many of the neurotransmitters present in mammals (18). As a result, EtOH might have a comparable effect on planarian synaptic transmission, warranting the use of EtOH in future studies on the role of the nervous system in intestinal regeneration.

To directly interfere with neural signaling at the transcriptional level, specific targets were selected based on the cell-type transcriptome atlas published by Fincher *et al.,* who sequenced the transcriptomes of all *S. mediterranea* cell types, including those previously unknown (29). From this database, five genes known to be involved in the neural control of intestinal homeostasis were identified as potential

targets for RNA interference: choline O-acetyltransferase (CHAT), cholinergic receptor nicotinic alpha 3 (CHRNA3), synaptotagmin I (SYT1), and nitric oxide synthase 1 adaptor protein (NOS1AP) from the cluster of non-ciliated neurons; and transient receptor potential cation channel subfamily A1 (TRPA1) from the cluster of ciliated neurons. Out of this selection we were able to optimize the smed-chat probe. Choline O-acetyltransferase catalyzes the synthesis of acetylcholine (ACh) from acetyl CoA and choline at cholinergic synapses. From literature we know that ACh is the major excitatory neurotransmitter in the ENS, and is a crucial neurotransmitter in both the CNS and PNS. In the gut, ACh is involved in the regulation of intestinal motility and epithelial homeostasis. Because flatworms do not have a circulatory system and rely on diffusion for nutrient exchange, their intestinal anatomy is vital for survival. Nishimura *et al.* revealed that cholinergic neurons are widely distributed in the planarian nervous system, including the brain, ventral nerve cords, optic nerves, and pharyngeal nerve plexus (30). This is reflected by the reduced brain size after RNAi and loss of eyes in most of the samples. Also the significant reduction in motility indicates the importance of acetylcholine signaling for mobility in planaria. In addition, we found that overall regeneration was reduced in planaria in whom ChAT was silenced. These effects were more pronounced after 2 weeks as compared to 1 week of injection. Whether this is due to the presence of residue chAT protein or incomplete transcriptional silencing is unclear. To confirm this qPCR can be applied to quantify chat expression in the future. We also examined the intestinal anatomy after full regeneration. The planarian intestine has a single anterior and two posterior primary branches, from these secondary, tertiary, and quaternary branches emerge toward the sides. Although we did not label the epithelial lining, based on the 6G10 intestinal muscle staining we found that chat-RNAi samples had a decreased secondary branch formation. This reduces the exchange surface and consequently limits the diffusion of nutrients. These results suggest that neurotransmitters, like ACh, may be involved in intestinal regeneration. Therefore, implicating neural control in this process.

A second target for specific interference were the voltage-gated sodium channels in neurons, which were blocked via the pharmacological agent tetrodotoxin (TTX). This binds to the ion channels in nerve cell membranes and blocks the passage of sodium ions into the neuron. TTX exposure resulted in impaired regeneration and moreover, underdeveloped intestinal branches, as shown with the 6G10 staining. These results correlate with the effects we observed after RNAi knock-down of ChAT, producing similar images of decreased secondary branch formation. In contrast, Zattara *et al.* found that TTX-treated annelids appeared to regenerate normally. They proposed a rescue mechanism via the presence of multiple types of sodium channels from which one or more may be TTX-insensitive (31). TTX is regularly used in vertebrate models to inhibit neuronal firing. However, in planarian literature few studies have been published that report TTX toxic effects on *S. mediterranea*, or use the neurotoxic compound to study neural signaling. The only example of TTX exposure with planaria in literature comes from two studies where TTX is assessed as a possible immobilizing agent, but without success.

To summarize, we produced similar data by interfering at multiple different levels with neuronal signaling, indicating that the nervous system does play a role in intestinal regeneration. Knock-down of choline acetyltransferase (neurotransmitter ACh production) or Na-channel blockage resulted in reduced secondary branch formation during intestinal regeneration. Which neural signal determines neoblast differentiation into intestinal cell types is still to be answered. Several candidates have been put forward in recent years including neurotransmitters such as Ach and nitric oxide, growth factors, EGFR 4 (epidermal growth factor receptor 4), and neurotrophins like BDNF (brain derived neurotrophic factor), GDNF (glial cell derived neurotrophic factor), FGF (fibroblast growth factor), or AGP (anterior gradient protein). All these targets have been implicated to be involved in neural signaling during regeneration. However, there are still a lot of ambiguities concerning the complex neural signaling for intestinal regeneration.

CONCLUSION

Our results suggest that a functioning nervous system is necessary for normal intestinal regeneration. We provide the first evidence of the

involvement of neuronal cues of intestinal regeneration in *Schmidtea mediterranea*. In the future, there is a need for more in depth mechanistic and molecular information. Looking for RNAi targets in the ciliated neurons could be interesting, because these cilia are present in the pharynx and probably in the intestine itself. Monitoring regeneration after damage, f.e. via EtOH injections, and how neuronal signals induce intestinal differentiation remains unanswered. Nevertheless, my study shows that using *Schmidtea mediterranea* as a model system for intestinal regeneration provides new opportunities that combine a high regenerative capacity with *in vivo* research and state-of-the-art molecular techniques.

REFERENCES

1. Pellettieri J. Regenerative tissue remodeling in planarians - The mysteries of morphallaxis. Seminars in cell & developmental biology. 2019;87:13-21.
2. Gehart H, Clevers H. Tales from the crypt: new insights into intestinal stem cells. Nature reviews Gastroenterology & hepatology. 2019;16(1):19-34.
3. Camilleri M. Leaky gut: mechanisms, measurement and clinical implications in humans. Gut. 2019;68(8):1516-26.
4. Cryan JF, O'Riordan KJ, Sandhu K, Peterson V, Dinan TG. The gut microbiome in neurological disorders. The Lancet Neurology. 2020;19(2):179-94.
5. Puzan M, Hosic S, Ghio C, Koppes A. Enteric Nervous System Regulation of Intestinal Stem Cell Differentiation and Epithelial Monolayer Function. Scientific reports. 2018;8(1):6313.
6. Bjerknes M, Cheng H. Modulation of specific intestinal epithelial progenitors by enteric neurons. Proceedings of the National Academy of Sciences. 2001;98(22):12497-502.
7. Pirotte N, Leynen N, Artois T, Smeets K. Do you have the nerves to regenerate? The importance of neural signalling in the regeneration process. Developmental Biology. 2016;409(1):4-15.
8. Klimovich AV, Bosch TCG. Rethinking the Role of the Nervous System: Lessons From the Hydra Holobiont. BioEssays : news and reviews in molecular, cellular and developmental biology. 2018;40(9):e1800060.
9. Forsthoefel DJ, Newmark PA. Emerging patterns in planarian regeneration. Current opinion in genetics & development. 2009;19(4):412-20.
10. Tanaka EM, Reddien PW. The cellular basis for animal regeneration. Dev Cell. 2011;21(1):172-85.
11. Birkholz TR, Van Huizen AV, Beane WS. Staying in shape: Planarians as a model for understanding regenerative morphology. Seminars in cell & developmental biology. 2019;87:105-15.
12. Bischof J, Day ME, Miller KA, LaPalme JV, Levin M. Nervous system and tissue polarity dynamically adapt to new morphologies in planaria. Developmental Biology. 2020;467(1):51-65.
13. Forsthoefel DJ, James NP, Escobar DJ, Stary JM, Vieira AP, Waters FA, et al. An RNAi screen reveals intestinal regulators of branching morphogenesis, differentiation, and stem cell proliferation in planarians. Dev Cell. 2012;23(4):691-704.
14. Bon-Frauches AC, Boesmans W. The enteric nervous system: the hub in a star network. Nature reviews Gastroenterology & hepatology. 2020;17(12):717-8.
15. Walsh KT, Zemper AE. The Enteric Nervous System for Epithelial Researchers: Basic Anatomy, Techniques, and Interactions With the Epithelium. Cellular and Molecular Gastroenterology and Hepatology. 2019;8(3):369-78.
16. Lowe JR, Mahool TD, Staehle MM. Ethanol exposure induces a delay in the reacquisition of function during head regeneration in Schmidtea mediterranea. Neurotoxicology and teratology. 2015;48:28-32.
17. Ross KG, Omuro KC, Taylor MR, Munday RK, Hubert A, King RS, et al. Novel monoclonal antibodies to study tissue regeneration in planarians. BMC Developmental Biology. 2015;15(1):2.
18. Cebrià F. Organization of the nervous system in the model planarian Schmidtea mediterranea: an immunocytochemical study. Neuroscience research. 2008;61(4):375-84.

19. Guo T, Peters AH, Newmark PA. A Bruno-like gene is required for stem cell maintenance in planarians. Dev Cell. 2006;11(2):159-69.
20. van der Flier LG, Clevers H. Stem cells, self-renewal, and differentiation in the intestinal epithelium. Annual review of physiology. 2009;71:241-60.
21. Jørgensen HA. Ethanol-Induced Effects on the Central Nervous System: A Short Review. Nordisk Psykiatrisk Tidsskrift. 1989;43(4):295-301.
22. Hanna L, McGee J, Srinivasan D, Staehle M. Ethanol Affects the Progression of Planarian Head Regeneration in a Time-Dependent Manner. The FASEB Journal. 2015;29(S1):1018.5.
23. Stevenson CG, Beane WS. A low percent ethanol method for immobilizing planarians. PLoS One. 2010;5(12):e15310-e.
24. Seitz HK, Simanowski UA, Homann N, Waldherr R. Cell proliferation and its evaluation in the colorectal mucosa: effect of ethanol. Z Gastroenterol. 1998;36(8):645-55.
25. Baguñá J. Mitosis in the intact and regenerating planarian Dugesia mediterranea n.sp. I. Mitotic studies during growth, feeding and starvation. Journal of Experimental Zoology. 1976;195:53-64.
26. Crews FT, Nixon K, Wilkie ME. Exercise reverses ethanol inhibition of neural stem cell proliferation. Alcohol. 2004;33(1):63-71.
27. Luo J, Miller MW. Growth factor-mediated neural proliferation: target of ethanol toxicity. Brain Research Reviews. 1998;27(2):157-67.
28. Deitrich RA, Dunwiddie TV, Harris RA, Erwin VG. Mechanism of action of ethanol: initial central nervous system actions. Pharmacological reviews. 1989;41(4):489-537.
29. Fincher CT, Wurtzel O, de Hoog T, Kravarik KM, Reddien PW. Cell type transcriptome atlas for the planarian Schmidtea mediterranea. Science. 2018;360(6391):eaaq1736.
30. Nishimura K, Kitamura Y, Taniguchi T, Agata K. Analysis of motor function modulated by cholinergic neurons in planarian dugesia japonica. Neuroscience. 2010;168(1):18-30.
31. Zattara EE, Turlington KW, Bely AE. Long-term time-lapse live imaging reveals extensive cell migration during annelid regeneration. BMC developmental biology. 2016;16:6-.

Acknowledgements – I am grateful for the guidance of professor Boesmans and professor Smeets during my internship and the writing process. I thank the members of the zoology research group at UHasselt for help with protocol optimizations. Special thanks to Julie Tytgat for assistance with all aspects of my thesis; Vincent Jaenen and Martijn Heleven for providing assistance with confocal microscopy and TTX experiments.

Author contributions – Prof. dr. Smeets and prof. dr. Boesmans conceived the research. CS designed and performed experiments and data analysis. JT supported optimization of immunostainings. CS wrote the paper. All authors carefully edited the manuscript.

SUPPLEMENTS

Tabel 1: Overview of protocols tested for immunostainings. Green labelled outcome indicates final protocol, pink labelled outcome indicates optimization in progress, and red labelled outcome indicates failed protocols. Abbreviations: WM, whole-mount; AB, antibody; SDS, Sodium Dodecyl Sulfate; FA, formaldehyde; Red, reduction solution; Me, methanol; 488 refers to second antibody Alexafluor goat anti-mouse 488.

	How	Fixation	Blocking 1	1e AB	Blocking 2	2e AB	Outcome
6G10	WM	HCl-Carnoy-Me	2h	1:200	3h	488 (1:400)	
		NAc-FA-Me-ProtK	3h	1:200	1h	488 (1:400)	
		NAc-FA-Red-Me-ProtK	3h	1:200	1h	488 (1:400)	
		NAc-FA-Me	3h	1:200	1h	488 (1:400)	
				1:50			
				1:10			
		NAc-FA-SDS-Me	3h	1:200	1h	488 (1:400)	
				1:50			
				1:10			
		NAc-FA-SDS	3h	1:200	1h	488 (1:400)	
				1:50			
				1:10			
		NAc-FA	3h	1:200	1h	488 (1:400)	
				1:50			
				1:10			
	Coupe	/	2h	1:200	/	488 (1:400)	
1H6	WM	NAc-FA-Red-Me-ProtK	1h	1:1000	1h	488 (1:400)	
Anti-p-TYR	WM	HCl-methacarn-Red-Me	8h	1:500	1h	488 (1:400)	
		HCl-methacarn-ProtK-Me	8h	1:500	1h	488 (1:400)	
		HCl-methacarn-Red-ProtK-Me	8h	1:500	1h	488 (1:400)	
		HCl-methacarn-Me	8h	1:500	ON	488 (1:400)	
				1:200			
				1:100			
				1:50			
	Coupe	/	2h	1:500	/	488 (1:400)	
2C4	WM	NAc-FA	4h	1:1000	1h	488 (1:400)	
6C8	WM	HCl-FA-ProtK	3h	1:100	1h	488 (1:400)	
				1:500			
		NAc-FA	1h	1:1000	1h	488 (1:400)	
			3h				
			8h		ON		
			ON				
		HCl-FA-ProtK	1h	1:1000	1h	488 (1:400)	
			3h				
			8h		ON		
			ON				